IEEE Access
Multidisciplinary | Rapid Review | Open Access Journal

Received January 17, 2022, accepted January 26, 2022, date of publication January 31, 2022, date of current version February 14, 2022.

Digital Object Identifier 10.1109/ACCESS.2022.3147821

Ebola Optimization Search Algorithm: A New Nature-Inspired Metaheuristic Optimization Algorithm

OLAIDE NATHANIEL OYELADE[1], ABSALOM EL-SHAMIR EZUGWU[1], TEHNAN I. A. MOHAMED[1], AND LAITH ABUALIGAH[2,3]

[1]School of Mathematics, Statistics, and Computer Science, University of KwaZulu-Natal, Pietermaritzburg Campus, Pietermaritzburg, KwaZulu-Natal 3201, South Africa
[2]Faculty of Computer Sciences and Informatics, Amman Arab University, Amman 11953, Jordan
[3]School of Computer Sciences, Universiti Sains Malaysia, George Town, Pulau Pinang 11800, Malaysia

Corresponding author: Absalom El-Shamir Ezugwu (ezugwua@ukzn.ac.za)

ABSTRACT Nature computing has evolved with exciting performance to solve complex real-world combinatorial optimization problems. These problems span across engineering, medical sciences, and sciences generally. The Ebola virus has a propagation strategy that allows individuals in a population to move among susceptible, infected, quarantined, hospitalized, recovered, and dead sub-population groups. Motivated by the effectiveness of this strategy of propagation of the disease, a new bio-inspired and population-based optimization algorithm is proposed. This study presents a novel metaheuristic algorithm named Ebola Optimization Search Algorithm (EOSA) based on the propagation mechanism of the Ebola virus disease. First, we designed an improved SIR model of the disease, namely SEIR-HVQD: Susceptible (S), Exposed (E), Infected (I), Recovered (R), Hospitalized (H), Vaccinated (V), Quarantine (Q), and Death or Dead (D). Secondly, we represented the new model using a mathematical model based on a system of first-order differential equations. A combination of the propagation and mathematical models was adapted for developing the new metaheuristic algorithm. To evaluate the performance and capability of the proposed method in comparison with other optimization methods, two sets of benchmark functions consisting of forty-seven (47) classical and thirty (30) constrained IEEE-CEC benchmark functions were investigated. The results indicate that the performance of the proposed algorithm is competitive with other state-of-the-art optimization methods based on scalability, convergence, and sensitivity analyses. Extensive simulation results show that the EOSA outperforms popular metaheuristic algorithms such as the Particle Swarm Optimization Algorithm (PSO), Genetic Algorithm (GA), and Artificial Bee Colony Algorithm (ABC). Also, the algorithm was applied to address the complex problem of selecting the best combination of convolutional neural network (CNN) hyperparameters in the image classification of digital mammography. Results obtained showed the optimized CNN architecture successfully detected breast cancer from digital images at an accuracy of 96.0%. The source code of EOSA is publicly available at https://github.com/NathanielOy/EOSA_Metaheuristic.

INDEX TERMS Ebola virus, metaheuristic algorithm, optimization problems, constrained benchmark functions, image classification, convolutional neural network.

I. INTRODUCTION

Ebola virus represents the virus causing the Ebola virus disease (EVD). The disease was first so named in the Democratic Republic of the Congo (DRC) in 1976. A widespread catastrophic outbreak was reported in late 2013 in the West African regions, including Sierra Leone, Liberia, Mali, Nigeria, and Senegal. It is widely reported that the virus made its entry into the human population through consumption or contact with infected animals such as fruit bats [1]–[3]. This animal-to-human infection led to person-to-person infection, becoming an epidemic across the West African region.

Contrary to the novel corona virus (COVID-19), the EVD person-to-person transmission occurs only when the infected

The associate editor coordinating the review of this manuscript and approving it for publication was Zhenzhou Tang.

person exhibits some form of signs and symptoms associated with Ebola. This transmission is aided by contact with any form of body fluid of an infected person. A healthy person comes in contact with infected objects since the Ebola virus can survive on dry surfaces such as doorknobs and countertops for several hours [4], [5]. The hemorrhagic disease, known to be notoriously fatal, has been reported to have mortality rates ranging from 25% to 90%, with an average of 50% mainly due to fluid loss rather than blood loss [6], [7]. Although the experimental Ebola vaccine proved highly protective against EVD, the transmission rate from the infected to the susceptible population is alarming. The high survival rate of EBOV in body fluids, including breast milk, saliva, urine, semen, cerebrospinal fluid, aqueous humor, blood, blood derivatives, and detected in amniotic fluid, tears, skin swabs, and stool by reverse transcription (RT)-PCR, presents a very high infection and transmission rate. This implies that a one-time virus entry into a susceptible population through a single individual has a high propagation rate.

A close study of the propagation strategy of the EVD and the resulting propagation model inspired the metaheuristic algorithm proposed in this study. Deriving computational solutions from natural phenomena has promoted a field of computing referred to as nature-inspired computing. A broader view of this aspect of computing may well relate to the field of Artificial Intelligence (AI) and Computational Intelligence (CI), where computational systems are designed by synthesizing behaviors of organisms or natural phenomena [8]–[10]. Metaheuristic algorithms are nature-inspired optimization solutions with high performance. They often require low computing capacity, which has successfully solved complex real-life problems in engineering, medical sciences, and sciences, especially in areas concerning swarm intelligence based algorithms [11]–[20]. These optimization algorithms are designed without specific reference to a particular problem. They are often categorized by performing a local or global search, handling single-solutions or whole populations, using memory, and adopting a greedy or iterative search process. The techniques often achieve near-optimal solutions to large-scale optimization problems due to their highly flexible manner of operation and ability to learn quickly owing to their natural or biological systems from which their designs were inspired.

A subfield of natural computation consists of biology-inspired techniques, also referred to as bio-inspired algorithms or computational biology. These techniques are stochastic, far from the design of deterministic heuristics. This feature has made it possible to represent the biological evolution of nature, hence capable of being used as a global optimization solution. Recently, bio-inspired optimization algorithms have helped support machine learning to address the optimal solutions to complex problems in science and engineering [21]. The bio-inspired algorithms combine biological concepts with mathematics and computer sciences and are classified as Evolutionary Algorithms (EA), Biology, and Swarm Intelligence (SI). Although the last two categories are often combined and referred to as swarm intelligence, not all bio-inspired algorithms have the swarm feature. Examples of evolutionary algorithms are Genetic Algorithms (GA) [22], Genetic Programming (GP), Differential Evolution (DE), the Evolution Strategy (ES), Coral Reefs Optimization Algorithm (CRO) [23], and Evolutionary Programming (EP). Examples of SI-based algorithms are: food foraging behavior of honeybees Artificial Bee Colony (ABC) [24], [25], echolocation ability Ant-lion Optimizer (ALO), luciferin induced glowing behavior Bees Algorithm (BAO), Bat Algorithm (BOA) [26], hunting behavior Barnacles Mating Optimizer (BMO), swarming around hive by honey bees Cuckoo Optimization Algorithm (COA), echo-cancellation Cuckoo Search Optimization (CSO) [27], hunting behavior and social hierarchy Dolphin Echolocation Optimization (DEO), social interaction and food foraging Dragonfly algorithm (DFA), Static and dynamic swarming behavior Deer Hunting Optimization (DHO), Pollination process of flowers Fire-fly Algorithm (FFA), Food foraging behavior Hunting search (FFO), bubble-net hunting Fruit Fly Optimization Algorithm (FOA), obligate brood parasitic behavior Flower-Pollination Algorithm (FPA), navigation and foraging behaviors Grasshopper Optimization Algorithm (GOA), spiral flying path of moth Glowworm Swarm Optimization (GSO), cuckoos' survival efforts Grey Wolf Optimizer (GWO) [28], flashing light patterns Moth-Flame Optimization (MFO), Mating behavior Manta Ray Foraging Optimizer (MRFO), Hunting behavior of humans SailFish optimizer (SFO), Group hunting behavior Salp Swarm Algorithm (SSA), and Hunting mechanism of Whale Optimization Algorithm (WOA) [29]. Others are Blue Monkey Optimization (BMO) [30], Arithmetic Optimization Algorithm (AOA) [31]–[33], Aquila Optimizer (AO) [34], Reptile Search Algorithm (RSA) [35], and Sandpiper Optimization Algorithm (SOA) [36].

These EA and SI-based algorithms have demonstrated good performance in solving real-world complex combinatorial problems, which are considered a fundamentally vital and critical task. In addition, studies have shown their capability to efficiently scale up to handle large-scale problems as opposed to traditional optimization methods, which are more effective for small-scale problems [37]. Further research in bio-inspired computing areas will lead to achieving similar and better new optimization algorithms capable of solving modern-day optimization problems. Our study showed that exploring the propagation model of diseases with endemic and pandemic natures may yield an outperforming optimization algorithm with interesting performance in solving real-world optimization problems. This study considered that optimization algorithms' exploration and exploitation phases are practically coupled into the natural order and strategy of propagation of these diseases. Studies confirm that finding a good balance between exploitation and exploration of the problem search space for an optimization algorithm determines its ability to find a globally optimal solution [38], [39]. The exploration phase often allows for finding

candidate solutions that are not neighbor to the current solution, while exploitation maintains its search in the neighborhood. Hence, we found a balance of the two scenarios in the disease propagation model for escape from a local optimum without neglecting good solutions in the neighborhood.

In this study, we propose a novel metaheuristic algorithm referred to as the Ebola Optimization Search Algorithm (EOSA), inspired by the Ebola virus disease and its propagation model (a preprint has previously been published [40]). We derived the novel algorithm through a careful study of our implementation of the SIR model of the disease. Particularly, our algorithm's novelty brought into metaheuristic design lies in the mechanism to balance between the exploration and exploitation phases. Secondly, the algorithm demonstrates an inherent ability to use a dynamic mechanism to update solutions as they transit through susceptible profitably, infection, quarantine, recovered, and hospitalized compartments. Initialization of solutions in the population follows the natural pattern of the disease through the application of a stochastic model. To quantitatively measure how fit a given solution is in solving the problem, give intuitive results, and discover the best or worst candidate solution, the resulting optimization algorithm is investigated on about forty-seven (47) classical benchmark optimization functions [41] and more than thirty (30) CEC functions [42]. In summary, the main contributions of this research are as follows:

i. An improved SIR model of Ebola disease and a modified mathematical model is designed to aid the proposed algorithm.
ii. We design a new nature-inspired metaheuristic algorithm using the models in (i).
iii. Applied EOSA to optimize the hyperparameters of a CNN architecture to image classification problem detecting breast cancer.
iv. Several experiments are conducted using over 89 mathematical optimization problems, including the classical benchmark functions and IEEE-CEC test suite, which are considered challenging test problems in the literature to evaluate the efficiency of the proposed EOSA.
v. Validation of the obtained numerical results using statistical analysis test further supports the superiority claim of the proposed EOSA optimization method over the existing state-of-the-art metaheuristic algorithms.

The rest of the paper is organized as follows. Section 2 provides an overview of the Ebola virus diseases. The proposed propagation model, mathematical model, and algorithmic design for the EOSA algorithm are given in Section 3. Section 4 details the benchmark functions applied to evaluate the performance of the proposed algorithm. Also, this section lists and discusses the parameterization and assignment of initial values used for experimentation. A discussion on results obtained is presented in Section 5, including numerical simulations that support the proposed propagation model. A detailed comparative analysis of the performance of EOSA and similar algorithms is also presented in the section. In Section 6, we give concluding remarks on how our novel optimization algorithm fits in the literature, its real-life applicability, and perspectives for future works.

II. RELATED WORK

This section summarises the Ebola virus disease, its propagation technique, and relevant SIR-based models that support this study. Also, considering the nature of the optimization algorithm proposed in this study which shares some principles of biology, we review studies that have developed bio-inspired optimization algorithms.

A. THE EBOLA VIRUS (EBOV) AND EBOLA VIRUS DISEASES (EVD): THE PROPAGATION MECHANISM

Ebola viruses result in what is known as the Ebola virus disease (EVD) once they successfully infect the host, suggesting victimization of the host. They are classified among the family of Filoviridae viruses, which are recognized by their different shapes of short or elongated branched filaments sizing up to 14,000 nanometers in length [6]. About six different species of the EBOV have been reported to exist. Bundibugyo Ebola virus, Ebola-Zaire virus, Tai Forest Ebola virus, and Sudan Ebola virus account for large flare-ups or outbreaks in Africa.

Exposure of a human individual to the virus through pathogenic agents or a contaminated environment initiates a population-based infection and after that, propels the spread of the disease. Direct contact with infected individuals spurs the propagation and spread of the virus. This contact relies on broken skin or mucous membranes in the eyes, nose, mouth, or other openings. It is assumed that such openings in the human body allow for body fluids (e.g. urine, saliva, sweat, faeces, vomit, breast milk, amniotic fluid, blood, and semen) bearing the virus to be transmitted to other susceptible individuals. Another host to the Ebola virus, which may transmit the disease to a healthy or susceptible individual, is a contaminated environment. An environment, such as medical equipment, clothes, bedding, and other related utensils, is considered contaminated if the body fluid of an infected individual has been spilt within or upon such an environment or object. Whereas an infected individual and a contaminated environment appear to have enhanced the propagation of EVD, infected animals consumed by humans have also been shown to propagate the disease [43]. These animals include bats, chimpanzees, fruit bats, and forest antelope, often hunted for food. Another propagative mechanism of the EBOV is culturally driven by burial practices in most affected populations and regions, with transmission occurring through contact with infected dead bodies. Meanwhile, note that the Ebola virus is not propagated through the air.

The application of different strategies, including case-based management approach, surveillance and contact tracing, quarantine of infected cases, infection prevention and control practices, and safe burial rites, has been adopted to revive and survive infected cases. However, infected cases remain positive while the virus remains in their blood. The infection and propagation rate of the EBOV presents an

appealing computational solution to numerous problems and so motivates the design of the proposed metaheuristic algorithm. While it appears that the solutions for mitigating the spread of the virus are suggestive of scaling down the infection rate, we argue that some other factors are still contributory to the propagation model. For instance, it is widely reported that the time-scale from symptom onset to death is an average of 10 days in 50–90% of cases [44].

To formalize and apply the propagation model of EBOV, we review some susceptible-infection-recovery (SIR) models. This is necessary for mainstreaming the concept proposed in the study. An interesting SIR model, based on EBOV, combining agent-based and compartmental models, has been presented [5]. The authors suggested that the hybrid model can switch from one paradigm to another on a stochastic threshold. The agent-based model consists of Susceptible (S), Infected (I), Hospitalized (H), Recovered (R), Funeral (F), and Dead (D). The Exposed (E) item was added to make up seven (7) compartments in the compartmental model. The SIR-based model was proposed to model the movement of individuals in a population from one compartment to another in both paradigms. For instance, individuals may move from Susceptible (S), Infected (I), to Hospitalized (H), based on a pre-existing computed rate. One external compartment considered in the literature is the influence of EBOV-carrying animals like bats. The assumption made was that since these animals can infect the human population without them (the animals) becoming ill, they present a reservoir-like mechanism for the virus in the SIR model.

Furthermore, the authors assumed that the rate of infection and hospitalization between infected individuals who will recover or die is the same, the deceased individual is buried in unsafe practices, and that recovered individuals are removed from the system. This SIR model presents a foundation for the modeling and implementation of the optimization algorithm proposed in this study. We considered that the compartments defined by Tanade *et al.* (year) work demonstrate the possibility to monitor and simulate the propagation model of the EBOV for the optimization task in our study.

In related work, Berge *et al.* (year) also modeled the propagation model of EBOV using the SIR-type model. The novelty of the study was the addition of the role of the indirect environmental transmission on the dynamics of EVD and to assess the effect of such a feature on the long run of the disease [45]. The authors showed that factoring direct and indirect transmission of EBOV into an SIR model promotes a system where the virus always exists in a population, increasing the propagation rate. Taking a cue from the novelty of this work in addition to that of Tanade *et al.* (year), we adapted the model proposed in this study to support the concept of direct and indirect transmission promoted by Berge *et al.* (year). Both studies supported their SIR models with mathematical models and further simulation to validate the performance of their model.

Similarly, Yet [46] successfully represented the basic interactions between EBOV and wild-type Vero cells in vitro . Rafiq *et al.* (year) also proposed the SEIR model, which mathematical model supported demonstrating the dynamics and illustrating the stability pattern of the Ebola virus in the human population. Their mathematical model is in the form of a couple of linear differential equations. The authors applied their SEIR model to study the disease-free equilibrium (DFE) and endemic equilibrium (EE) to report the stability of the model. Another study investigating the spread of EVD in India is [47] hoping to find EBOV transmission in the region through an SEIR model. Using ordinary differential equations, the study represented the SEIR model as a mathematical model and simulated it using a spatiotemporal epidemiology modeler (STEM). Rachah and Torres [47] also applied a mathematical model to study the outbreak of EBOV and eventually the EVD. The novelty of this study is the addition of vaccination to the proposed model. We found this appealing considering the role of the vaccine in stemming the tide of the infected population. Whereas most SEIR approaches have often adopted the stochastic method for the simulation of the model, Okyere *et al.* [48] considered using a deterministic scheme for designing models and studying the infection rate of EBOV. As an improvement to the work of Rachah and Torres (year), which factored in vaccination, the study also captured treatment and educational campaigns as time-dependent control functions in the SEIR model proposed.

This study developed a comprehensive SEIR-based model with more compartments, considering the above review. The proposed SEIR model factored in the notion of quarantine, which we found to play a role in curtailing EBOV propagation. In addition, we modeled the SEIR model to allow for the inclusion of the influence of vaccines in the pace of the growth of infection among a given population. The SEIR model was then formulated using an ordinary differential equation. This presented a good understanding of the design of the proposed metaheuristic algorithm. The resulting model is detailed in Section 3 and its supporting mathematical model.

B. METAHEURISTIC OPTIMIZATION ALGORITHMS: BIOINSPIRED-BASED ALGORITHMS

Bio-inspired optimization algorithms represent a class of metaheuristic algorithms whose principles are inspired by biology and natural phenomena. Generally, these algorithms have successfully been applied to solve different optimization problems in engineering and other related fields [49]. This category of algorithms exploits the basic processes of nature and then translates them into rules or procedures, which are then modeled computationally for solving complex real-life problems [50]–[57]. They are mostly population-based algorithms, and examples of such are Satin Bowerbird Optimizer (SBO), Earthworm Optimisation Algorithm (EOA), Wildebeest Herd Optimization (WHO), Virus Colony Search (VCS), Slime Mould Algorithm (SMA), Invasive Weed Colonization Optimization (IWO), Biogeography-Based Optimization (BBO), Coronavirus Optimization

Algorithm (COA), Emperor Penguin Salp Swarm Algorithm (ESA). Although evolutionary-based algorithms like GA and DE and swarm-based algorithms like PSO, WOA, and ABC share some characteristics of a biology-inspired algorithm, we have chosen to limit our review to those listed.

ESA is a hybrid of two phenomena drawn from the Salp Swarm Algorithm and Emperor Penguin. The behaviour of the two creatures is modelled to achieve ESA. Comparing the proposed algorithm with similar metaheuristic algorithms, authors [58] revealed that the algorithm demonstrated good performance based on sensitivity, scalability, and convergence analyses. Coronavirus Optimization Algorithm (COA) based on its propagation strategy, and another variant, namely Coronavirus Herd Immunity Optimizer (CHIO) based on human immunity, has been proposed. The COA proposed in [59] and CHIO in [60] leveraged infection and herd immunity. The effectiveness of COA was evaluated by applying it to the design of the convolutional neural network (CNN) problem, while CHIO proved robust at real-world engineering problems. Earthworm Optimisation Algorithm (EOA), also referred to as EWA, is a metaheuristic algorithm whose inspiration was drawn from the reproductive nature of the earthworm [61]. The mechanism involves two reproduction strategies where the first strategy allows for a parent to reproduce only one offspring while the other allows for more than one offspring. This reproducibility is controlled by the Cauchy mutation approach allowing for crossover operators.

Biogeography-Based Optimization (BBO) solves its optimization problem by implementing the geographical distribution and positioning of biological organisms [62]. Alluding to the fact that BBO's features are similar to those of GAs, the authors drew inspiration from the original mathematical model of the biogeography of organisms to derive BBO. Experimentation shows that BBO successfully solved real-world sensor selection problems to detect the status of aircraft engines and a selection of 14 benchmark optimization functions. Invasive Weed Optimization (IWO) is an optimization algorithm that has been widely applied to numerous problems and is based on numerical stochastic optimization algorithms learnt from the invasive nature of weeds [63]. The aggressive invasive nature of weeds allows for colonizing the environment against other economically viable plants. Knowing that this is a disadvantage agricultural-wise, the concept has benefited from solving optimization problems. The resulting algorithm was successfully applied to engineering problems, namely optimization and tuning the robust controller and well-known benchmark functions. Satin Bowerbird Optimization (SBO) is a biology-based optimization algorithm whose inspiration was drawn from the phenomenon of the male satin bowerbird's capability of attracting the female for breeding. [64]. The Satin Bowerbird Optimizer (SBO) algorithm has been successfully applied to the optimization problem in estimating the efforts needed to develop software. Wildebeest Herd Optimization (WHO) is a bio-inspired metaheuristic algorithm rooted in the behavior of wildebeest when searching for food [65]. A lookout for grazing land often guides the search with a high vegetation density. The WHO exploits the following natural characteristics of herds of wildebeest to achieve its performance: local search capability of wildebeest due to limited eyesight, look out for sparsely grazed region to avoid crowded grazing, exploitation of past experiences to explore regions with a high density of vegetation, starvation avoidance strategy deployed through the transition to new regions or location, and lastly, herd-based movement to avoid predators.

The propagation strategy of the virus in the host environment can sometimes be aggressive and often overwhelm the whole environment. Authors [39] proposed Virus Colony Search (VCS) motivated by this mechanism. The VCS exploration and exploitation phases leverage the propagation approach of the virus through diffusion or infection of the host environment. VCS has been successfully applied to the classic benchmark functions and the modern CEC2014 benchmark functions and real-life problems regarding energy consumption management [66]. Slime Mould Algorithm (SMA) optimization algorithm is based on a fungus named slime mould, which inhabits cold and humid places [67]. The algorithm's authors explored the nutritional stage, also referred to as plasmodium of the organism, for its design. They have a mechanism for multiple food sources and at the same time form a connected venous network so that they can even grow to more than 900 square centimeters depending on food availability. Using a mathematical model, the authors were able to simulate the process of producing positive and negative feedback of the propagation wave of slime mould based on bio-oscillator to form the optimal path for connecting food with excellent exploratory ability and exploitation propensity. SMA was successfully applied to solve engineering problems, including cantilever, welded beam, and pressure vessel structure problems.

While we acknowledge that these are not exhaustive and many new optimization algorithms inspired by natural processes are being developed, they provide the reader with a general understanding of the inspiration and principle behind such a class of algorithms.

III. METHODOLOGY: EOSA METAHEURISTIC ALGORITHM

Understanding how an SEIR-based model works in the propagation of a disease is important to appealing for the design of an optimization algorithm. Hence, this section presents an improved SEIR model based on recent literature on EVD. Secondly, a presentation of the procedural flow of EOSA and the corresponding flow chart are presented and discussed. Lastly, to formalize the proposed optimization algorithm, we represent the SEIR model using a mathematical model and then the algorithm.

A. SIR MODEL OF EOSA

SEIR-based models designed for EVD have been proposed in the literature to monitor both direct and indirect propagation of the disease in the affected population [45] and [5]. This study adopts and adapts two relevant models from

the existing SEIR models by identifying and adding new compartments perceived as omitted. These compartments are the contaminated environment serving as a reservoir of the virus, vaccination and quarantine, denoted by PE, V, and Q, respectively. This became necessary considering that the Ebola virus and disease are not propagated among the human population except by an individual infected from the reservoir. Also, the roles played by vaccination and quarantined infected individuals have impacted on the propagation rate of the virus. This perception is supported by recent studies [68]–[71]. This therefore necessitated the re-modeling of the propagation model which now yielded the SEIR-HDFVQ: Susceptible (S), Exposed (E), Infected (I), Recovered (R), Hospitalized (H), Death or dead (D), Funeral (F), Vaccinated (V), and Quarantine (Q). Also, in designing the model, we considered that an insignificant number of recovered cases might still retain the virus in their body fluid, which has potency for infecting healthy individuals [72]–[74]. Since this study's interest was to leverage the propagation model of the EVD for developing an optimization algorithm, it became necessary to explore all factors supporting increased infection.

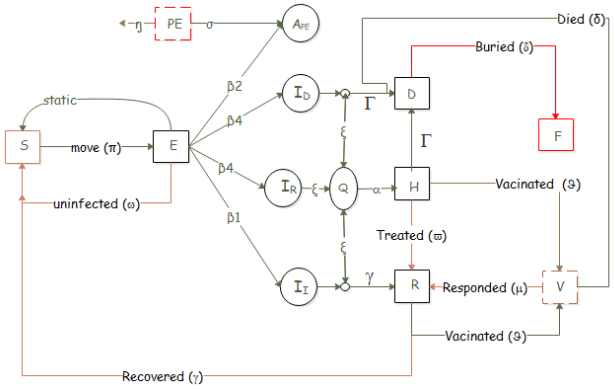

FIGURE 1. The SEIR-HDVQ propagation model of the proposed EOSA metaheuristic model.

The model of the SEIR-HDVQ is shown in Figure 1, and the listing of its parameters is presented in Table 1. The propagation of EVD is assumed to provide a suitable manner for solving some optimization problems considering its aggressive infection rate is overwhelming communities. The Figure assumes a population of susceptible individuals whose exposure could trigger the population of other subgroups. Exposed individuals, contaminated environments, and agent reservoirs can randomly draw arbitrary individuals from the susceptible into the category of infected, which may be due to exposure to any individual from the subgroups of the infected. Subgroups of infected individuals are infected from the dead individual, infected individual, recovered individual, contaminated environment, and agent-reservoir. We show that the virus has the potential of decaying in its contaminated environment. Furthermore, the propagation model shows that the infected cases could die without going to a hospital and recover without hospitalization. An assumption made in this study was classifying every vaccinated case as hospitalized. Also, we assumed that both the hospitalized (H) and non-hospitalized cases could transit into the dead (D). At the same time, those recovered (R) from vaccination (V) are returned to the susceptible (S).

TABLE 1. Notations and description for variables and parameters for SEIR-HDVQ.

Symbols	Data Type	Descriptions
S	Vector	Susceptible individuals
E		Exposed individuals
I		Infected individuals
H		Hospitalized infected individuals
R		Recovered infected individuals
D		Diseased from infection individuals
V		Vaccinated infected individuals
PE		Agents capable of infecting individuals
π	Scalar	Recruitment rate of susceptible human individuals
η		Decay rate of Ebola virus in the environment
α		Rate of hospitalization of infected individuals
Γ		Disease-induced death rate of human individuals
β_1		Contact rate of infectious human individuals
β_2		Contact rate of pathogen individuals/environment
β_3		Contact rate of deceased human individuals
β_4		Contact rate of recovered human individuals
γ		Recovery rate of human individuals
τ		Natural death rate of human individuals
δ		Rate of burial of deceased human individuals
ϑ		Rate of vaccination of individuals
ϖ		Rate of response to hospital treatment
μ		Rate response to vaccination
ξ		Rate of quarantine of infected individuals

The rates of change of variables or parameters applied in this study are summarized in Table 1. The values of most of these parameters are already predetermined by related studies on EVD and are detailed in Section 4.

B. FLOWCHART OF EOSA

1. Motivated by the performance of the SEIR-HDVQ model, we derived the design of the EOSA algorithm. The formalization of the EOSA algorithm is achieved from the following procedure: Initialize all vector and scalar quantities which are individuals and parameters: Susceptible (S), Infected (I), Recovered (R), Dead (D), Vaccinated (V), Hospitalized (H), and Quarantine (Q).
2. Randomly generate the index case (I_1) from susceptible individuals.
3. Set the index case as the global best and current best, and compute the fitness value of the index case.
4. While the number of iterations is not exhausted and there exists at least an infected individual, then
   a. Each susceptible individual generates and updates their position based on their displacement. Note that the further an infected case is displaced, the more the number of infections, so that short displacement describes exploitation, otherwise exploration.
      i. Generate newly infected individuals (nI) based on (a).
      ii. Add the newly generated cases to I.

b. Compute the number of individuals to be added to H, D, R, B, V, and Q using their respective rates based on the size of I.
c. Update S and I based on nI.
d. Select the current best from I and compare it with the global best.
e. If the condition for termination is not satisfied, go back to step 6.

5. Return global best solution and all solutions.

In Figure 2 below, the flow chart of the proposed EOSA metaheuristic algorithm is shown.

The flowchart presents the flow of process and information as a buildup from the procedure described above. The detailing shows the various levels of initialization and conditional checking. Also, the computation leading to the exploration and exploitation stages of the proposed EOSA metaheuristic algorithm are demonstrated. Lastly, the procedure for updating all subgroups is identified. In the following subsection, the algorithm's mathematical model, as it applies to the flowchart, is presented and discussed.

C. MATHEMATICAL MODEL OF EOSA

To update the positions of each exposed individual, Equation (1) applies:

$$mI_i^{t+1} = mI_i^t + \rho M\,(I) \tag{1}$$

where ρ represents the scale factor of displacement of an individual, mI_i^{t+1} and mI_i^t are the updated and original positions respectively at time t and $t+1$. $M(I)$ is the movement rate made by individuals and is defined thus:

$$M\,(I) = srate * rand\,(0,1) + M(Ind_{best}) \tag{2}$$

$$M\,(s) = lrate * rand\,(0,1) + M(Ind_{best}) \tag{3}$$

The exploitation stage is designed based on the assumption that the infected individual either stays within a distance of zero (0), or is displaced within a limit not exceeding *srate* - where *srate* denotes short distance movement. The exploration phase is founded on the fact that the infected individual moves beyond the average neighborhood range *lrate*. The consideration in this study is that the farther the displacement, the more the number of individuals in S are exposed to infection. Both cases are shown in Equations (2) and (3). The *srate* and *lrate* are regulated by a *neighborhood* parameter such that when *neighborhood* is >= 0.5, an individual has moved beyond the *neighborhood* leading to the mega infection; otherwise it remains within the *neighborhood,* which curbs infection.

1) INITIALIZATION OF SUSCEPTIBLE POPULATION

At the beginning, an initial population is generated by random number distribution whose initial positions are all zero (0). The individual is generated as shown in Equation (4). The $\boldsymbol{U_i}$ and $\boldsymbol{L_i}$ denote the upper and lower bounds respectively for the $\boldsymbol{i^{th}}$ individual, where I ranges from 1,2,3... N, in the population size.

$$individual_i = L_i + rand\,(0,1) * (U_i + L_i) \tag{4}$$

The selection of the current best is computed on the set of infected individuals in time t as seen in Equation (5):

$$bestS = \begin{cases} gBest, & fitness(cBest) < fitness\,(gBest) \\ cBest, & fitness\,(cBest) \geq fitness\,(gBest) \end{cases} \tag{5}$$

where ***bestS***, ***gBest*** and ***cBest*** all denote the best solution, global best solution, and current best solution at time ***t***; ***fitness*** represents the objective function applied to the problem. We distinguish ***gBest*** and ***cBest*** as infected individuals who are ***Superspreader*** and ***Spreader*** of the Ebola virus, respectively.

Update of Susceptible (S), Infected (I), Hospitalized (H), Exposed (E), Vaccinated (V), Recovered (R), Funeral (F), Quarantine (Q), and a system of ordinary differential equations govern dead (D) based on those in [45] and [5]. Differential calculus is a branch of calculus that is a branch in mathematics. The former deals with the rate of change of one quantity concerning another, while the latter deals with finding different properties of integrals and derivatives. In our case, the application of differential calculus intends to obtain the rates of change of quantities S, I, H, R, V, D, and Q with respect to time ***t***. Hence, the Equations (6)-(12) are as follows:

$$\frac{\partial S(t)}{\partial t} = \pi - (\beta_1 \mathrm{I} + \beta_3 \mathrm{D} + \beta_4 \mathrm{R} + \beta_2\,(\mathrm{PE})\,)\,S - (\tau \mathrm{S} + \Gamma \mathrm{I}) \tag{6}$$

$$\frac{\partial I(t)}{\partial t} = (\beta_1 \mathrm{I} + \beta_3 \mathrm{D} + \beta_4 \mathrm{R} + \beta_2\,(\mathrm{PE})\,\lambda)\,S - (\Gamma + \gamma)\,I - (\tau)\mathrm{S} \tag{7}$$

$$\frac{\partial H(t)}{\partial t} = \alpha \mathrm{I} - (\gamma + \varpi)\mathrm{H} \tag{8}$$

$$\frac{\partial R(t)}{\partial t} = \gamma I - \Gamma R \tag{9}$$

$$\frac{\partial V(t)}{\partial t} = \gamma I - (\mu + \vartheta)V \tag{10}$$

$$\frac{\partial D(t)}{\partial t} = (\tau \mathrm{S} + \Gamma \mathrm{I}) - \delta D \tag{11}$$

$$\frac{\partial Q(t)}{\partial t} = (\pi \mathrm{I} - (\gamma \mathrm{R} + \Gamma \mathrm{D})) - \xi Q \tag{12}$$

We assume that Equations (6-11) are *scalar functions*, meaning that each has one number as a value, which can be represented as a float. This is not far removed from some common scalar differential equations and their corresponding f functions, such as exponential growth of money or populations governed by scalar differential equations: $u' = \alpha u$, where u *is the* growth rate.

We determine the rate of change of the population of susceptible individuals and then apply it to the current size of the susceptible vector to obtain the number of susceptible individuals at time ***t***. The same procedure is applied to compute the set of individuals in vectors I, H, R, V, D, and Q using rates described in Table 1. This study assumes the

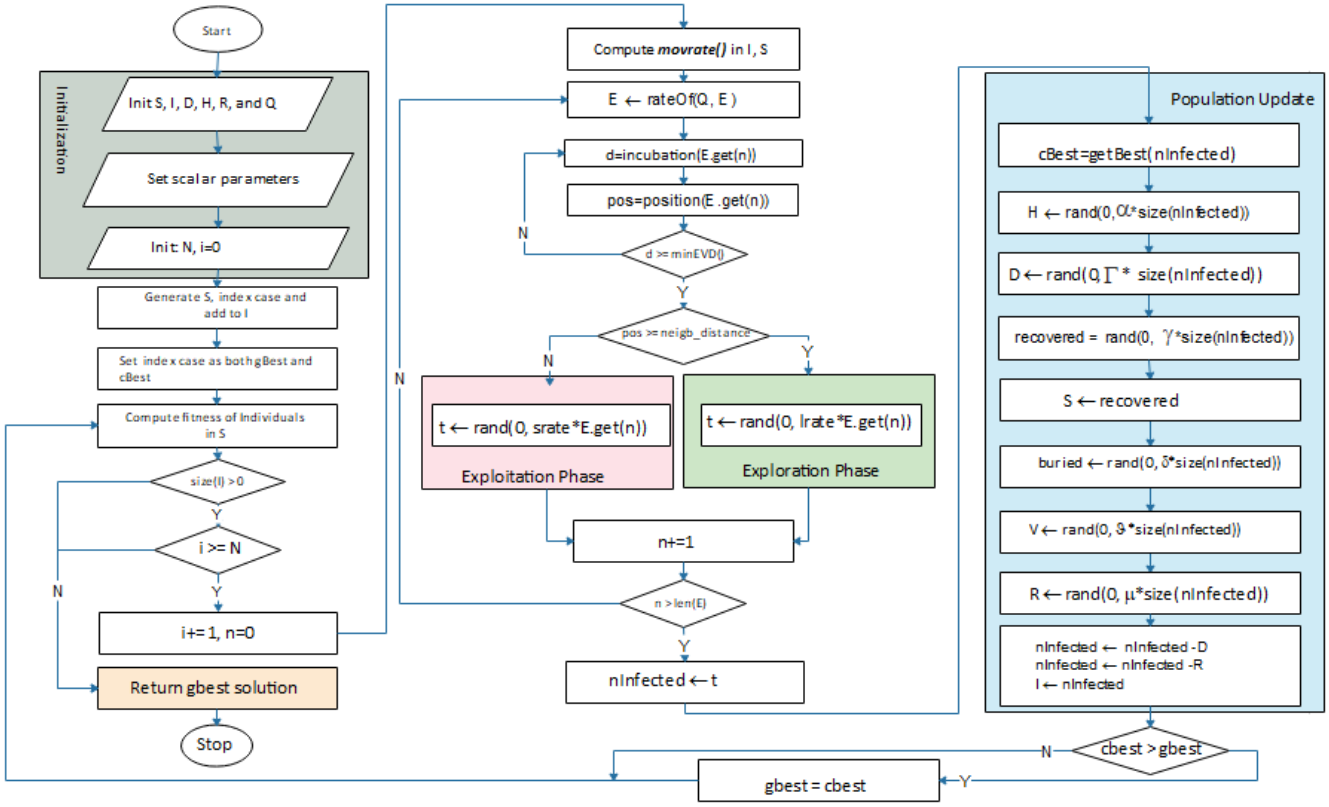

FIGURE 2. Flowchart of the proposed EOSA metaheuristic algorithm.

initial conditions S(0) = S0, I(0) = I0, R(0) = R0, D(0) = D0, P(0) = P0, and Q(0) = Q0 where our t follows after the epoch, and δ in equation (11) is for the burial rate. Equation (12) models the rate of quarantine of infected cases of Ebola.

D. ALGORITHM DESIGN OF EOSA

The pseudo-code of the proposed EOSA metaheuristic algorithm is shown in Algorithm 1. Lines 1-7 of the algorithm show the initialization phase. To naturalize the concept that not all infected cases have the potency for recruiting newly infected individuals, on Line 8 we show that some I are drawn into quarantine status so that the remaining fraction of I infect S population. On Lines 10-24, new infections are generated from S and then added to I. Since R, V, H, and V are only derivable from I, Lines 25-29 of Algorithm 1 generate individuals using corresponding equations of subgroups. Logically, recovered and dead cases need to be removed from I before the next iteration. In our demonstration, recovered cases are added back to S while dead individuals are replaced in S with new cases – to promote the idea of new births as shown on Lines 29-31. Finally, the best solution is computed, and the termination criterion is checked so that when satisfied, the algorithm terminates, otherwise return to Line 7. To demonstrate the usability of the algorithm, we follow on in the next section for experimental setup, configurations, and parameter definition.

IV. EXPERIMENTAL SETUP

This section presents the computational environment applied for experimentation. First, we show the control parameter settings and variable assignment, then a listing of the benchmark functions applied to the algorithm, and finally detail the evaluation criteria.

A. CONFIGURATION OF THE EXPERIMENTAL SETUP

Exhaustive experimentation evaluated the proposed EOSA in a workstation environment with the following configurations: Intel (R) Core i5-7500 CPU 3.40GHz, 3.41GHz; RAM of 16 GB 64-bit Windows 10 OS for each configuration of the system on the network. A total of ten (10) existing metaheuristic algorithms were implemented and experimented with for comparative purposes with the EOSA algorithm. This study executed each algorithm twenty (20) times to ensure fairness in each algorithm's evaluation. Also, five hundred (500) epochs were covered in each run. The runs of 20 for each algorithm allowed computing the average values for all metrics.

B. PARAMETERS OF EOSA METAHEURISTIC ALGORITHM

The design and selection of EOSA's parameters and corresponding values assumed the natural definitions generated from those reported in the literature. In this study, we adopted the rates reported in studies that have extensively evaluated

Algorithm 1 EOSA metaheuristic algorithm

Result: Best solution
Input: objfunc, lb, ub, epoch, psize, evdincub
Output: solution, gbest

$S, E, I, H, R, V, Q, sols \leftarrow \emptyset$;
$S \leftarrow createSusceptibleIndvd(psize, S)$ *using* $Eq.4$;
$icase \leftarrow generatedIndexCase(S)$;
$gbest, cbest \leftarrow icase$;
while $e \leq epoch \wedge len(I) > 0$ **do**
  $Q \leftarrow rand(0, Eq.12 \times I)$;
  $fracI = I - Q$;
  for $i \leftarrow 1$ ***to*** $len(fracI)$ **do**
    $pos_i \leftarrow movrate()$ *using* $Eq.1$;
    $d_i \leftarrow rand()$;
    $newI \leftarrow \emptyset$;
    if $d_i > evdincub$ **then**
      $neighborhood \leftarrow prob(pos_i)$;
      if $neighborhood < 0.5$ **then**
        $tmp \leftarrow rand(0, Eq.7 \times I \times srate)$;
      end
      else
        $tmp \leftarrow rand(0, Eq.7 \times I \times lrate)$;
      end
      $newI+ \leftarrow tmp$;
    end
    $I+ \leftarrow newI$;
  end
  $h \leftarrow rand(0, Eq.8 \times I), H+ \leftarrow h$;
  $r \leftarrow rand(0, Eq.9 \times I), R+ \leftarrow r$;
  $v \leftarrow rand(0, Eq.10 \times h), V+ \leftarrow v$;
  $d \leftarrow rand(0, Eq.11 \times I), D+ \leftarrow d$;
  $I+ \leftarrow I - add(r, d)$;
  $S+ \leftarrow r$;
  $S- \leftarrow d$;
  $cbest = fitness(objfunc, I)$;
  if $cbest > gbest$ **then**
    $gbest = cbest$;
    $sols \leftarrow gbest$;
  end
end
return gbest, sols;

the SEIR models. These studies relied on the WHO data for the evaluation of their models. All these parameters have been described in Section 3, where the SEIR-HDVQ model was presented.

In Table 2, the initial value for each parameter is defined. Considering the stochastic nature of EOSA, which is characteristic of biology-based optimization algorithms, values for some parameters are randomly assigned. The problem size applied for all experimentation is fixed at one hundred (100). We note that these values remain fixed for all experiments on the benchmark functions.

TABLE 2. Notations and description of variables and parameters for SEIR-HDVQ.

Symbols	Descriptions	Range
π	Recruitment rate of susceptible human individuals	0.1
β_1	Contact rate of infectious human individuals	0.1
β_2	Contact rate of pathogen individuals/environment	0.1
β_3	Contact rate of deceased human individuals	0.1
β_4	Contact rate of recovered human individuals	0.1
Γ	Disease-induced death rate of human individuals	Random values initialized within the range of 0-1
γ	Recovery rate of human individuals	
η	Decay rate of Ebola virus in the environment	
α	Rate of hospitalization of infected individuals	
τ	Natural death rate of human individuals	
δ	Rate of burial of deceased human individuals	
ϑ	Rate of vaccination of individuals	
ϖ	Rate of response to hospital treatment	
μ	Rate response to vaccination	
ξ	Rate of quarantine of infected individuals	

C. BENCHMARK FUNCTIONS

To evaluate the effectiveness of the proposed EOSA metaheuristic algorithm, this study applied forty-seven (47) standard and high dimensional functions for this purpose. These functions are listed in Table 3 and are subsequently used for performance comparison with similar metaheuristic algorithms. We listed the names, mathematical representation, and range of the functions. We also evaluated the algorithm using the IEEE-CEC benchmark functions to demonstrate exhaustive experimentation.

Whereas many test functions are continuous, they are categorized into four (4). Test functions characterized by unimodal, convex, and multidimensional forms are first class. They represent a class of test functions with interesting functions with cases capable of slowing down convergence or even yielding a poor convergence. The resulting convergence trails from such a slow pace to a single global extremum. The second class consists of test functions of type multimodal, two-dimensional with few local extremes. This test function category appeals to situations where we intend to test the quality of standard optimization procedures in an anticipated hostile environment. This hostile environment describes problem domains with only a few local extremes with a single global one. The third and fourth classes represent a list of test functions known as multimodal two-dimensional with a huge number of local extremes, and multimodal multidimensional, with a huge number of local extremes. It has been shown that these test functions work well for situations where the quality of intelligent and resistant optimization algorithms are tested [41], [75]–[79].

D. EVALUATION METHOD

The following metrics were considered in the performance evaluation: mean, median, standard deviation, maximum values, minimum or worst values, average values, overall convergence time, and average execution time. In addition to

TABLE 3. Standard benchmark functions used for the experimentation: Dimensions (D), Multimodal (M), Non-separable (N), Unimodal (U), Separable (S).

ID	Function name	Range	Model of the function	D	Type	Min
F1	Ackley	[−32, 32]	$f(x) = -20e^{\left(-0.2\sqrt{\frac{1}{n}\sum_1^n x_i^2}\right)} - -e^{\left(\frac{1}{n}\sum_1^n \cos(2\pi x_i)\right)} + 20 + e^{(1)}$	30	MN	0
F2	Alpine	[−10, 10]	$f(x) = \sum_{i=1}^{n} \lvert x_i \sin(x_i) + 0.1x_i \rvert$	N	MN	0
F3	Brown	[-1, 4]	$f(x) = \sum_{i=1}^{n-1} (x_i^2)^{(x_{i+1}^2+1)} + (x_{i+1}^2)^{(x_i^2+1)}$	N	UN	0
F4	Bent Cigar	[-100,100]	$f_{20}(x) = x_1^2 + 10^6 \sum_{i=2}^{D} x_i^2$	N	MS	0
F5	Composition1	[-100,100]	g1=Rosenbrock's Function F29 g2=High Conditioned Elliptic Function F15 g3=Rastrigin's Function F27	5		
F6	Composition2	[-100,100]	g1=Ackley's Function F1 g2=High Conditioned Elliptic Function F15 g3=Griewank Function F10 g4=Rastrigin's Function F27	3		
F7	Dixon and Price	[-10, 10]	$f_{18}(x) = 10^6 x_1^2 \sum_{i=2}^{D} x_i^2$	30	UN	0
F8	Discus Function	[−100, 100]	$f(x) = (x_1 - 1)^2 + \sum_{i=2}^{n} i(2x_i^2 - x_{i-1})^2$	N	U	
F9	Fletcher–Powel	[−100, 100]	$f(x) = 100\left\{\left[x_3 - 10\theta(x_1,x_2)\right]^2 + \left(\sqrt{x_1^2 + x_2^2} - 1\right)^2\right\} + x_3^2$ Where $2\pi\theta(x_1,x_2) = \begin{cases} \tan^{-1}\frac{x_2}{x_1}, & if x_1 \geq 0 \\ \pi - \tan^{-1}\frac{x_2}{x_1}, & otherwise \end{cases}$	N	MN	0.0001
F10	Griewank	[−600, 600]	$f(x) = 1 + \sum_{i=1}^{n} \frac{x_i^2}{1400} - \prod_{i=1}^{n} \cos(\frac{x_i}{\sqrt{i}})$	30	MN	0
F11	Generalized Penalized Function 1	[-50, 50]	$f(x) = \frac{\pi}{n} X \left\{10sin^2(\pi y_i) + \sum_{i=1}^{n-1}(y_i - 1)^2 [1 + 10sin^2(\pi y_{i+1})] + (y_n - 1)^2\right\} + \sum_{i=1}^{n} u(x_i, a, k, m)$ Where $y_i = 1 + \frac{1}{4}(x_i + 1)$, $u(x_i,a,k,m) = \begin{cases} k(x_i - a)^m & if\ x_i > a \\ 0 & if -a \leq x_i \leq a \\ k(-x_i - a)^m & if\ x_{i<-a} \end{cases}$ a=10, k=100, m=4	n	M	0
F12	Generalized Penalized Function 2	[-5.12, 5.12]	$f(x) = 0.1\ X \left\{sin^2(3\pi x_1) + \sum_{i=1}^{n-1}(x_i - 1)^2 [1 + sin^2(3\pi x_{i+1})] + (x_n - 1)^2[1 + sin^2(2\pi x_n)]\right\} + \sum_{i=1}^{n} u(x_i, a, k, m)$ Where $u(x_i,a,k,m) = \begin{cases} k(x_i - a)^m & if\ x_i > a \\ 0 & if -a \leq x_i \leq a \\ k(-x_i - a)^m & if\ x_{i<-a} \end{cases}$ a=5, k=100, m=4	N	M	0
F13	Holzman 2 function	[-100,100]	$f(x) = \sum_{i=1}^{n} ix_i^4$	N		
F14	HGBat	[-100,100]	$f_{23}(x) = \left\lvert (\sum_{i=1}^{D} x_i^2)^2 - (\sum_{i=1}^{D} x_i)^2 \right\rvert^{1/2} + (0.5\ \sum_{i=1}^{D} x_i^2 + \sum_{i=1}^{D} x_i)/_D + 0.5$	30	M	
F15	High Conditioned Elliptic	[-100,100]	$f_{23}(x) = \sum_{i=1}^{D} (10^6)^{\frac{i-1}{D-1}} x_i^2$	N		
F16	Hybrid1	[-100,100]	g1 : Zakharov Function F45 g2 : Rosenbrock Function F29 g3: Rastrigin's Function F27	3	UN	0
F17	Hybrid2	[-100,100]	g1 : High Conditioned Elliptic Function F15 g2 : Ackley's Function F1 g3: Rastrigin's Function F27 g4: HGBat Function F14 g4: Discus Function F8	3	MN	0
F18	Inverted Cosine Mixture	[-1,1]	$f_{14}(x) = 0.1n - (0.1\ \sum_{i=1}^{n} \cos(5\pi x_i) - \sum_{i=1}^{n} x_i^2)$	N	MS	-0.1x(n)
F19	Lévy 3 function	[−10, 10]	$f(x) = \sum_{i=1}^{n-1}\left[0.5 + \frac{sin^2(\sqrt{100x_i^2 + x_{i+1}^2}) - 0.5}{1 + 0.001(x_i^2 - 2x_ix_{i+1} + x_{i+1}^2)^2}\right]$	N		
F20	Levy	[−10, 10]	$f_{12}(x) = \sum_{i=1}^{n}(x_i - 1)^2 [sin^2(3\pi x_{i+1})] + sin^2(3\pi x_1) + \lvert x_n - 1 \rvert [1 + sin^2(3\pi x_n)]$	2	MN	0
F21	Levy and Montalo	[−5, 5]	$f_{17}(x) = 0.1(sin^2(3\pi x_1)) + \sum_{i=1}^{n}(x_i - 1)^2(1 + sin^2(3\pi x_{1+1})) + (x_n - 1)^2(1 + sin^2(2\pi x_n))$	N	MS	0
F22	Noise	[−1.28, 1.28]	$f_7(x) = \sum_{i=1}^{n} x_i^4 + random[0,1)$	N		
F23	Pathological function	[-100,100]	$f(x) = \sum_{i-1}^{5} icos((i-1)x_1 + i) \sum_{j=1}^{5} jcos((j+1)x_1 + j)$	N	MN	0
F24	Perm	[-20, 20]	$f(x) = \sum_{k=1}^{n}\left[\sum_{i=1}^{n}(i_k + \beta)((\frac{x_i}{i})^k - 1)\right]^2$	N	MN	0
F25	Powel	[-4, 5]	$f(x) = (x_1 + 10x_2)^2 + 5(x_3 + x_4)^2 + (x_2 - 2x_3)^4 + 10(x_1 - x_4)^4$	N	UN	0
F26	Quartic	[-128, 128]	$f_6(x) = \sum_{i=1}^{n} ix_i^4$	30	MS	0
F27	Rastrigin	[−5.12, 5.12]	$f_9(x) = \sum_{i=1}^{n}[x_i^2 - 10\cos(2\pi x_i) + 10]$	30	MN	0

TABLE 3. *(Continued.)* **Standard benchmark functions used for the experimentation: Dimensions (D), Multimodal (M), Non-separable (N), Unimodal (U), Separable (S).**

F28	Rotated hyperellipsoid	[−100, 100]	$f_3(x) = \sum_{i=1}^{n}\left(\sum_{j=1}^{i} x_j\right)$	N	U	0
F29	Rosenbrock	[−30, 30]	$f(x) = \sum_{i=1}^{n-1}[100\,(x_{i+1} - x_i^2)^2 + (x_i - 1)^2]$	30	UN	0
F30	Schwefel 2.26	[-500, 500]	$f(x) = \sum_{i=1}^{n}[-x_i \sin(\sqrt{\lvert x_i \rvert})]$	N	MS	−418.983
F31	Schwefel 1.2	[−100, 100]	$f(x) = \sum_{i=1}^{n}(\sum_{j=1}^{i} x_j)^2$	30	UN	0
F32	Schwefel 2.22	[−100, 100]	$f(x) = \sum_{i=1}^{n}\lvert x_i \rvert + \prod_{i=1}^{n}\lvert x_i \rvert$	30	UN	0
F33	Schwefel 2.21	[−100, 100]	$f(x) = \max\{\lvert x_i \rvert, 1 \le i \le n\}$	N	US	0
F34	Sphere	[−100, 100]	$f_1(x) = \sum_{i=1}^{n} x_i^2$	30	US	0
F35	Step	[−100, 100]	$f(x) = \sum_{i=1}^{n}(floor(x_i) + 0.5)^2$	30	US	0
F36	Sum/SumSquares Function	[−10, 10]	$f(x) = \sum_{i=1}^{n} i x_i^2$	30	US	0
F37	Sum-Power	[−1, 1]	$f_8(x) = \sum_{i=1}^{n}\lvert x_i \rvert^2$	N	US	0
F38	Sum of Different Power	[-100,100]	$f_{21}(x) = \sum_{i=1}^{d}\lvert x_i \rvert^{i+1}$	N	US	0
F39	SR-F4	[-100,100]	Shifted and Rotated Bent Cigar Function	N		
F40	SR-F38	[-100,100]	Shifted and Rotated Sum of Different Power Function	N		
F41	SR-F45	[-100,100]	Shifted and Rotated Zakharov Function	N		
F42	SR-F29	[-100,100]	Shifted and Rotated Rosenbrock's Function	N	MN	0
F43	SR-F27	[-100,100]	Shifted and Rotated Rastrigin's Function	N	MS	0
F44	Wavy 1	[-100,100]	$f(x) = \sum_{i=1}^{n} x_i^2 + (\sum_{i=1}^{n} 0.5 i x_i)^2 + (\sum_{i=1}^{n} 0.5 i x_i)^4$	2	MS	0
F45	Zakharov	[−5, 10]	$f(x) = \frac{1}{n}\sum_{i=1}^{n} 1 - \cos(10x_i)\, e^{-\frac{1}{2}x_i^2}$	10	UN	0
F46	Salomon	[−100, 100]	$f_{19}(x) = 1 - cos\left(2\pi \sqrt{\sum_{i=1}^{n} x_i^2}\right) + 0.1\sqrt{\sum_{i=1}^{n} x_i^2}$	N	MN	0
F47	Weierstrass Function	[-0.5, 0.5]	$f(x) = \sum_{i=1}^{D}(\sum_{i=0}^{20}[0.5^k \cos(2\pi . 3^k (x_i + 0.5))])$	50	MN	0

these, we applied the outcome of the proposed EOSA and related optimization algorithms to statistical tests to evaluate their performance in terms of convergence to determine algorithms capable of generating similar final solutions.

V. RESULT AND DISCUSSION

A detailed performance evaluation of the outcome of the experimentation carried out in Section 4 is presented and discussed in this Section. First, we study the performance of the proposed SEIR-HDVQ model to determine how it effectively describes the natural phenomenon. Performance evaluation uses the values obtained from applying the optimization algorithms to the test functions. Compared with other methods, the proposed algorithm's performance is statistically analysed. Also, the application of the algorithm to medical image classification using convolutional neural network (CNN) architectures is presented.

A. SIMULATION OF EVD PROPAGATION BASED ON SEIR-HDVQ MODEL

The simulation of the proposed SEIR-HDVQ model applied to EOSA during experimentation is demonstrated. The result

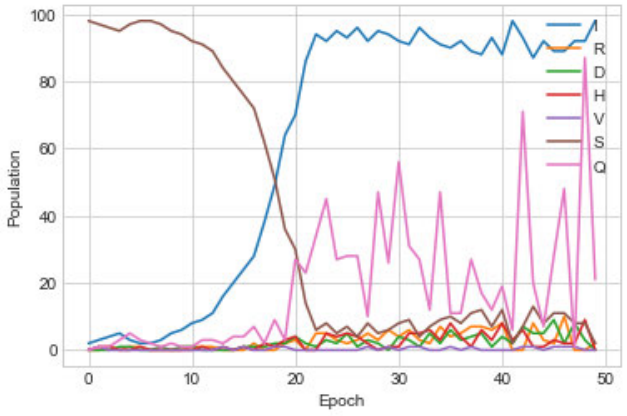

FIGURE 3. An estimated propagation curve of the Ebola virus and disease based on the simulation with randomly generated data while experimenting with the EOSA optimization algorithm. The curve illustrates variations in the values of Susceptible (S), Infected (I), Recovered (R), Hospitalized (H), Dead (D), Vaccinated (V), and Quarantine (Q) using the SEIR-HDVQ model.

is reported to investigate the naturalization tendency of the SEIR-HDVQ model as obtained in the real-life propagation model for the EVD and EBOV.

In Figure 3, the curves for Susceptible (S), Infected (I), Recovered (R), Hospitalized (H), Dead (D), Vaccinated (V), and Quarantine (Q) are captured so that they show the rate at which each compartment rises and falls within a period of fifty (50) epochs. In the Figure, we observed that the early phase of the infection outbreak rose against the susceptible population. The Figure also revealed the response to the rising infection rate through quarantine measures, such that as infection rose, the number of quarantine individuals also increased – a measure to stem the outbreak. Meanwhile, we noticed that recovery and death rate curves wobbled along with infection and quarantine.

B. PERFORMANCE OF EOSA WITH SIMILAR METAHEURISTIC ALGORITHMS USING CLASSICAL FUNCTIONS

The performance of EOSA was compared with nine (9) different optimization algorithms, namely Artificial Bee Colony (ABC), Whale Optimization Algorithm (WOA), Butterfly Optimization Algorithm (BOA), Particle Swarm Optimization (PSO), Differential Evolution (DE), Genetic Algorithm (GA), Henry Gas Solubility Optimization Algorithm (HGSO), Blue Monkey Optimization (BMO), and Sandpiper Optimization Algorithm (SOA). The experimentation, which was executed for five hundred (500) iterations and twenty (20) different runs, applied forty-seven (47) standard benchmark functions.

Table 4 lists the outcome for the best, worst, mean, median, and standard deviation for each of the 47 functions. An overview of the results showed that although EOSA outperformed most of the algorithms in most cases for the 47 functions, some interesting differences were noticed, which appears to group the outcome into two. Whereas EOSA demonstrated a very close performance compared to ABC, WOA, BOA and PSO, we observed that EOSA's outcome compared with DE, GA, and HGSO was significantly better. For example, for F1-4, F6-7, F12, F14-15, F18, F20-23, F2, F29-30, F32-36, F38, F40-43, and F46-47, EOSA clearly achieved the best values in all cases. However, in the cases of F5, F9-11, F13, F16-17, F19, and F25-26, EOSA was outperformed based on WOA and BOA, ABC, WOA, and PSO, ABC, BOA and PSO, ABC and PSO, ABC, ABC, WOA, and BOA, respectively. Meanwhile, we found some situations for the 47 functions where there was no clear superiority of EOSA over similar algorithms, neither were the similar algorithms able to demonstrate clear superiority. These cases are found in F28, F31, F37, F39, F44, and F45, where we observed that ABC and PSO beat EOSA, beaten by WOA, BOA and PSO, ABC, matched values in ABC and PSO, beaten by WOA, and beaten by ABC, WOA, and PSO respectively

As shown in Table 4 for the 47 functions, the values obtained for the worst revealed a strong competition between EOSA and ABC, WOA, BOA, and PSO. We discovered that only in the cases of F3, F6, F12, F18, F22-23, F27, F29, F28, and F40-41 were the values of EOSA better than those listed earlier and also completely outperformed those same algorithms in the cases of F13, F21, F25, and F32. However, we noticed that the discrepancies reported by these algorithms compared to EOSA were not significantly large. Meanwhile, DE, GA, and HGSO maintained a significant variation in the values obtained for best and worst computations. This implied that the proposed EOSA algorithm and its competitive related algorithms (ABC, WOA, BOA, and PSO) performed significantly well over DE and GA. Meanwhile, we found the performance of SOA and HGSO very competitive with that of EOSA. For instance, when investigating the overall superiority of each algorithm compared with others, the following were observed: EOSA(12), ABC(4), WOA(1), BOA(1), PSO(1), DE(1), GA(2), BMO(0), HGSO(19), and SOA(21). This shows that both HGSO and SOA had more occurrences of superiority. Interestingly, when each method was compared with EOSA, the following were observed: ABC/EOSA(15/28), WOA/EOSA(5/28), BOA/EOSA(2/28), PSO/EOSA(4/28), DE/EOSA(0/28), GA/EOSA(0/28), BMO/EOSA(0/28), HGSO/EOSA(23/21), and SOA/EOSA(22/20).

We note that although other similar metaheuristics algorithms may compete with the EOSA method on the sets of the various mathematical benchmark functions tested in this study, it is noteworthy that the comparison with the selected algorithms showed that the performance of EOSA is very competitive.

To confirm the outstanding performance and superiority of the EOSA, the convergence curves of the history of solutions are graphed in Figure 4. The benchmark functions F1, F2, F3, F4, F7, F8, F20, F25, F26, F27, F43, and F45. We observed that in all cases, the curve of the plots descended appreciably. The implication is that the EOSA algorithm is a very competitive optimization algorithm that can discover optimum solutions in exploration and exploitation operations. To demonstrate the superiority of EOSA, when its convergence curve was plotted against those of state-of-the-art algorithms, we found that its solutions were significant.

The convergence of EOSA using the benchmark functions as compared with ABC, WOA, PSO, and GA was graphed and is illustrated in Figure 5. The Figures showed that in most cases, the best values for all the algorithms were descending from their initial peak values to a lower value as the training improved over some epochs. The graphing was achieved by obtaining the best values for each case of EOSA, ABC, WOA, PSO, and GA at 1, 50, 100, 200, 300, 400, 500 iteration points. The Figure confirms that the best values for GA are often larger than the others except in a few cases where ABC also has some large values. However, ABC, WOA, PSO, and the proposed EOSA do not just have low values for the best cases but appear to only drop in value for small fractions across all the iterations. This is why their rise and fall concerning their curves was not so pronounced compared to that of GA and sometimes ABC.

Perspective views of some selected functions, alongside the search history, are shown in Figures 6 and 7. Again,